



## Does dust change the clear sky top of atmosphere shortwave flux over high surface reflectance regions?

Falguni Patadia,<sup>1</sup> Eun-Su Yang,<sup>1</sup> and Sundar A. Christopher<sup>1,2</sup>

Received 8 May 2009; revised 24 June 2009; accepted 20 July 2009; published 13 August 2009.

[1] Using four stream radiative transfer calculations, satellite-derived aerosol optical thickness at 558 nm and top of atmosphere (TOA) broadband radiative fluxes we examine the effect of mineral dust aerosols on the clear sky TOA shortwave (0.3–5  $\mu\text{m}$ ) fluxes over the Saharan desert [30E–10W, 15N–30N]. Over very bright surfaces (surface albedo > 35%), the TOA shortwave flux, from both satellite measurements and model calculations, is nearly insensitive to the increase in dust optical thickness. Below this surface albedo value, known as the critical albedo, mineral dust aerosols show scattering effects and above this they show absorbing effects. Therefore, over desert regions with a large range of surface albedo values, scattering and absorbing effects compensate each other thereby making the TOA shortwave aerosol radiative effect rather small.  
**Citation:** Patadia, F., E.-S. Yang, and S. A. Christopher (2009), Does dust change the clear sky top of atmosphere shortwave flux over high surface reflectance regions?, *Geophys. Res. Lett.*, 36, L15825, doi:10.1029/2009GL039092.

### 1. Introduction

[2] North Africa is a source region for various aerosol types but it is especially noted for desert dust during the spring and summer seasons [Prospero *et al.*, 2002]. Nearly 700 Tg of dust aerosols are produced annually in the Saharan desert [Laurent *et al.*, 2008]. Due to the aridity of the desert regions, it is also noted for its high surface reflectance. Satellite remote sensing is the only viable method to obtain information on dust aerosols and their properties at such large spatial scales. A few ground measurements of aerosols exist over North Africa as part of the Aerosol Robotic Network (AERONET) program but it is limited in terms of spatial sampling. Several field campaigns have also been conducted to examine the role of dust primarily in climate related issues [e.g., Haywood *et al.*, 2008].

[3] Although the physical processes governing the aerosol radiative effects are well established, determining the sign and magnitudes of aerosol effects on climate has been challenging, especially in desert dust regions partly due to the high surface reflectivity and also due to the variation in aerosol properties in space and time. One of the important climate parameters is shortwave aerosol radiative effect at the top of atmosphere (TOA). Aerosol radiative effect in the shortwave is usually calculated as the clear sky TOA

shortwave flux (0.3–5  $\mu\text{m}$ ) subtracted by the flux under aerosol conditions and is called shortwave direct radiative effect (SWDRE). Since aerosols are brighter than ocean surface, they exert a negative SWDRE over oceans. Over bright surfaces, the sign and magnitude of the SWDRE is a complex function of aerosol and surface type and atmospheric conditions [Hsu *et al.*, 2004]. Dust aerosols are non-spherical in shape and their size distribution depends on factors such as parent soil type, wind velocity and ageing process [Grini and Zender, 2004]. For example, from the Dust and Biomass-burning Experiment (DABEX) [Haywood *et al.*, 2008] in Sahelian West Africa, Osborne *et al.* [2008] found that for a generic mineral dust size distribution in this region, the reduced two mode log-normal mode radii ( $r_{g0}$ ) are 0.075  $\mu\text{m}$  and 1.050  $\mu\text{m}$ . Their respective fractional contributions in terms of number are 0.983 and 0.017. They find a high single scattering albedo ( $\omega_0$ ) of around  $0.99 \pm 0.01$  at 0.55  $\mu\text{m}$ . However, dust aerosols could be mixed with absorbing aerosols such as those from biomass burning, thereby reducing the  $\omega_0$  of dust aerosols [Johnson *et al.*, 2008]. Also, larger dust particles can perturb the longwave radiation balance [Zhang and Christopher, 2003].

[4] Chen *et al.* [2009] note that high dust loading and intense solar radiation over high reflectance surfaces could cause a large aerosol radiative effect. Over land region, they calculate the change in TOA spectral albedo ( $d\alpha$ ) due to aerosols and suggest a 5% underestimation of global mean  $d\alpha$  when desert regions are neglected. In deriving the broadband TOA aerosol SWDRE over global land regions, Patadia *et al.* [2008] did not report the SWDRE for global desert regions due to noisy SWF-AOT relations in these regions. The goal of this paper is to examine whether dust aerosols change the TOA shortwave flux over high reflectance regions such as the Sahara desert under cloud free conditions and whether the SWDRE is significantly underestimated if dust radiative effects over bright regions are neglected. The cloud free TOA shortwave flux will be referred to as shortwave flux (SWF). We use aerosol optical thickness (AOT) at 558 nm (to characterize dust loading) and broadband shortwave fluxes from satellite measurements to characterize the SWDRE over North Africa (15–30N and 30E–10W; see Figure 1). We use the AOT estimated from combined Ozone Monitoring Instrument (OMI) and Multiangle Imaging Spectroradiometer (MISR) products [Christopher *et al.*, 2008] that is called estimated AOT (EAOT) and the SWF from the Clouds and the Earth's Radiant Energy System (CERES) product. The relation between AOT and SWF is further examined as a function of broadband surface albedo ( $\alpha_s$ ) from the Moderate resolution Imaging Spectroradiometer (MODIS). We also use 4-stream radiative transfer (RT) calculations to compare

<sup>1</sup>Department of Atmospheric Sciences, University of Alabama in Huntsville, Huntsville, Alabama, USA.

<sup>2</sup>Earth System Science Center, University of Alabama in Huntsville, Huntsville, Alabama, USA.

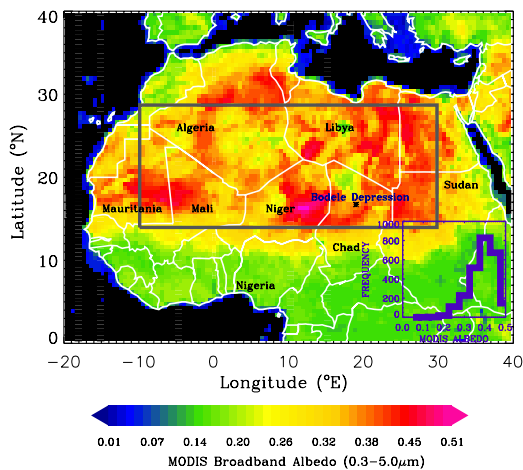


**Figure 1.** Area of study shown in the rectangle with the broadband surface albedos from the MCD43C3 Product for June–September, 2005. The inset shows the frequency distribution of surface albedo values for the region shown in the rectangle.

against the satellite-based AOT and SWF relationships and to determine SWDRE and the reasons for noisy AOT-SWF relations found over deserts in the previous study [Patadia *et al.*, 2008].

## 2. Data and Radiative Transfer Model

[5] Eight months of the OMI and MISR data (June–August, 2005–2006) is used over North Africa (Figure 1) to obtain EAOT values [Christopher *et al.*, 2008]. Over desert regions, the relative mean error between EAOT and AERONET AOT is on the order of 20% [Christopher *et al.*, 2008] and has been used to validate dust forecasting models [Greed *et al.*, 2008] successfully. The CERES single scanner footprint data set that reports broadband shortwave (0.3–5  $\mu\text{m}$ ) fluxes at a nadir spatial resolution of 20 km is used. Since the surface reflectance over the area of study varies markedly we examine the SWDRE of dust aerosols as a function of surface albedo. We use the 0.05 degree spatial resolution broadband black-sky (directional hemispherical or direct) surface albedo from MODIS Climate Modeling Grid (CMG) Albedo product (MCD43C3) [Schaaf *et al.*, 2002]. Figure 1 shows the area of study and the underlying broadband black-sky surface albedo used in this study. High albedo values are noted, as expected, over desert region including source regions such as the Bodele Depression, Lake Chad Basin and areas in Niger. Using the Total Ozone Monitoring Spectrometer (TOMS), Prospero *et al.* [2002] showed that most of the prominent and persistent dust sources in the Saharan desert are located north of 15° N and are related with topographic lows. Sand dunes, on the other hand, may be important sporadic sources of dust. However, there is considerable variability in albedo over the study region (see histogram in Figure 1). Albedo values range from 8%–50% but less than 1% of the study area has  $\alpha_s < 15\%$ , 5% of the area has  $\alpha_s < 20\%$  while 80% of the area has  $\alpha_s$  value within 25% and 40%. The rest of the area ( $\sim 7\%$ ) comprises of  $\alpha_s > 40\%$ . The mean surface albedo over the study region is 36%.

[6] A delta-four stream plane-parallel broadband radiative transfer (RT) model [Fu and Liou, 1993] was used to compute shortwave (0.2–4  $\mu\text{m}$ ) flux and SWDRE values for dust aerosols. The input parameters for this RT model include the  $\alpha_s$ , the default tropical atmosphere profiles [McClatchey *et al.*, 1971] of water vapor, temperature, other atmospheric constituents (e.g.,  $\text{O}_3$ ) and aerosol optical properties ( $\omega_0$ , extinction coefficient ( $\beta_{\text{ext}}$ ), and asymmetry factor ( $g$ )). In the model, AOT and  $\alpha_s$  are varied between 0.02–1.5 and 0.05–0.50 respectively.

[7] Dust aerosol sizes and other properties vary with space and time because they have widely varying compositions including quartz, various forms of clay and other minerals. For computational purposes, we use representative dust aerosol models from Hess *et al.* [1998] that has  $\omega_0$ ,  $\beta_{\text{ext}}$  and  $g$  values of 0.965, 0.665  $\text{km}^{-1}$  and 0.697 respectively between 0.2–0.7  $\mu\text{m}$ . From DABEX measurements, Osborne *et al.* [2008] report the dust  $\omega_0$ ,  $k_{\text{ext}}$  and  $g$  of  $0.99 \pm 0.02$ , 0.33  $\text{m}^2\text{g}^{-1}$  and 0.75 at 0.55  $\mu\text{m}$  respectively. Although the RT model was run for various dust types, only the representative dust model (chosen above) that best matched the results from satellite observations is shown here. Unlike shortwave flux computed from RT model, which is subject to variation with an assumed value of each input parameter, the CERES shortwave flux does not require any assumption on the value of each parameter.

## 3. Results and Discussion

[8] Figure 2a shows the relationship between CERES shortwave wave flux and the EAOT over the area of study. The data (shown in gray) appears rather noisy at first glance, although a general increase in SWF is seen as a function of AOT. Patadia *et al.* [2008] derived the SWDRE for global land regions and found similar noisy SWF-AOT relations over deserts. They noted that the change in shortwave flux is a combined effect of both the aerosol and the underlying surface properties. To further examine this in detail, we examine the effect of the surface albedo and desert dust aerosol properties on the shortwave flux and discuss the implications for estimating dust SWDRE over very bright regions.

### 3.1. Dependence of Flux on Surface Albedo and Aerosol Optical Thickness

[9] To examine the effect of surface albedo on the shortwave flux, we bin the CERES SWF according to various  $\alpha_s$  values. Figures 2a and 2b shows the relationship between CERES SWF and AOT (filled colored circles) and also between the modeled SWF and AOT (colored lines) as a function of surface albedo. Note that the modeled SWF agrees reasonably well with the CERES shortwave flux values (filled circles in Figure 2b) for the entire surface albedo range. Several interesting features can now be seen in Figures 2a and 2b. First, for any given AOT value, the backscattered SWF increases with increase in  $\alpha_s$ , as expected. Secondly, the effect of mineral dust in enhancing backscattered SWF can be seen only at low  $\alpha_s$  values (e.g.,  $\alpha_s < 20\%$ ) where the slope of the SWF-AOT relation is positive. Next, as  $\alpha_s$  increases, the slope of SWF-AOT relation decreases and becomes zero for  $35\% < \alpha_s \leq 40\%$ . For  $\alpha_s > 40\%$  there is a slight decrease in SWF with

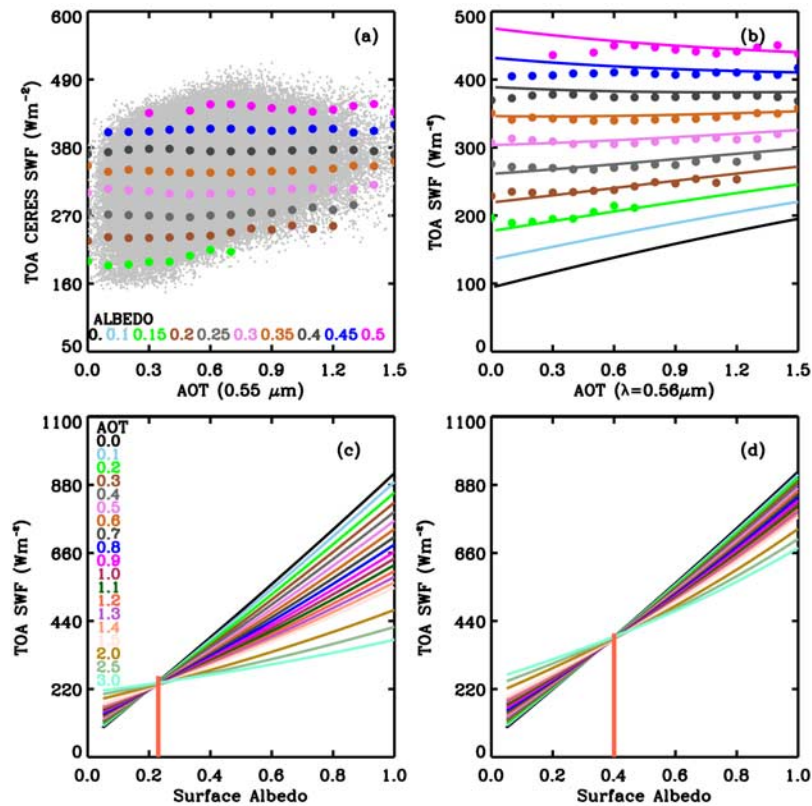


**Figure 2.** (a) Relationship between TOA shortwave flux (SWF) from CERES and estimated AOT (EAOT) from MISR and OMI. The filled circles show the SWF-AOT relation as a function of broadband (0.3–5.0  $\mu\text{m}$ ) surface albedo from MODIS. (b) Same as Figure 2a but colored lines depict results from the 4-stream radiative transfer model (RTM) calculations for nucleation mode mineral dust aerosols at  $\text{SZA} = 25^\circ$  and  $\text{VZA} = 0^\circ$ . (c) Variation of SWF with surface albedo as a function of AOT from RTM calculations for mineral dust in accumulation mode at  $\text{SZA} = 25^\circ$  and  $\text{VZA} = 0^\circ$ . The red line shows the critical albedo value. (d) Same as Figure 2c but for mineral dust in nucleation mode.

increase in AOT (negative slope). From Figures 2a and 2b it is apparent that for our study region, the  $\alpha_s$  value of 35–40% appears to be the critical albedo ( $\alpha_c$ ) below (above) which aerosol scattering (absorption) effect dominates [Liao and Seinfeld, 1998]. Thus, the variation in SWF should be interpreted as the combined response to both variations in  $\alpha_s$  and AOT. It is noted that surface albedo has a larger effect on the SWF as compared to AOT. This is because dust over desert offers a scene with low contrast and hence does not enhance the effective albedo of the scene substantially. This is the major reason for the noisy SWF-AOT relation and that there were no reported SWDRE values over desert regions in Patadia *et al.* [2008].

### 3.2. Dependence of Flux on Aerosol Properties and Solar Zenith Angle

[10] The top of atmosphere SWF is computed using the 4-stream RT model to examine its dependence on different dust types found over the desert regions. As an example, we show in Figures 2c and 2d how the critical albedo (see the vertical lines) changes for two different mineral dust models: one that is absorbing ( $\omega_0 = 0.87$ ,  $g = 0.74$  and  $\beta_{\text{ext}} = 0.99$  in visible) versus another that is more scattering ( $\omega_0 = 0.97$ ,  $g = 0.67$  and  $\beta_{\text{ext}} = 0.69$  in visible). The critical albedo at which the SWF is insensitive to AOT is lower for the absorbing aerosols compared to the scattering aerosols. Thus, the critical albedo depends on

the aerosol properties. Therefore, over desert regions with a mixture of different mineral dust types, there will be a large range of  $\alpha_s$  values for which SWF will show less response to changes in AOT.

[11] The SWF also changes with change in solar zenith angle. The RT model simulations show changes in the magnitude of SWF for varying SZAs ( $5^\circ$ ,  $25^\circ$  and  $40^\circ$ ). The change is more pronounced for higher surface albedo (20–40%) values as opposed to low surface albedo (5–20%). However all other relations including the critical albedo value remain unchanged for both aerosol types considered here (not shown).

### 3.3. Implications for Dust DRE

[12] The variation in SWF with AOT is of interest because of the SWDRE of aerosols; the sign and magnitude of which is uncertain [Intergovernmental Panel on Climate Change, 2007]. From Figures 2a or 2b the SWDRE of dust over deserts can be speculated. As discussed in section 3.1, for  $\alpha_s < \alpha_c$ , where the scattering effect dominates, the SWDRE at the TOA will be negative. At the critical albedo value ( $30\% < \alpha_s < 45\%$ ) where the SWF is constant for increasing AOT values, the SWDRE will be zero [Yoshida and Murakami, 2008]. For  $\alpha_s > \alpha_c$ , the aerosols predominantly absorb incident radiation and will cause positive SWDRE. Thus, depending on the range of surface albedo values, the net SWDRE of mineral dust will be a cancella-

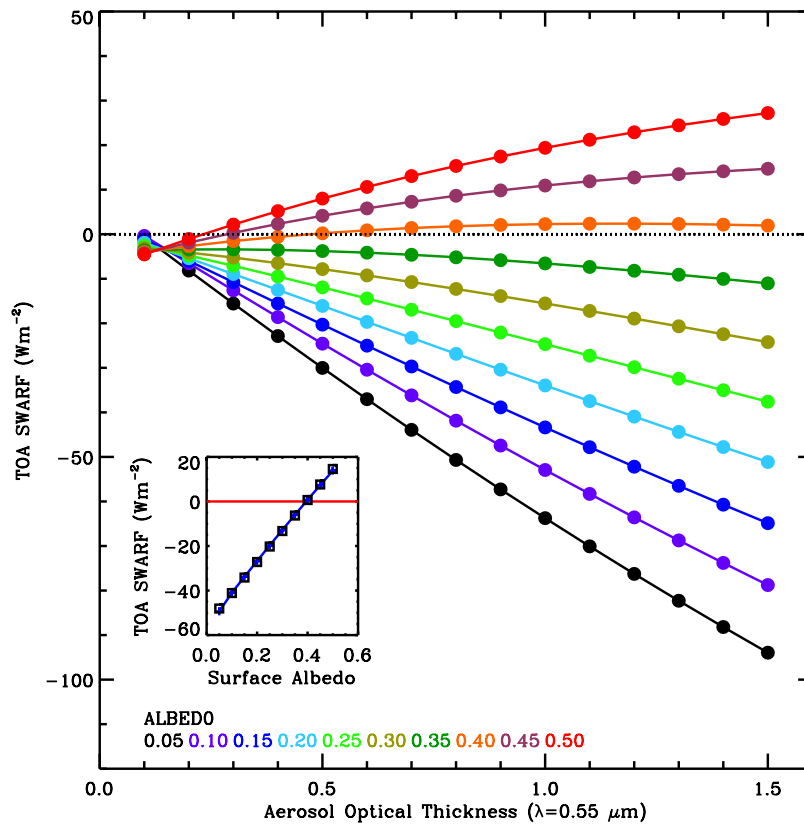


**Figure 3.** Relationship of TOA SWDRE of mineral dust and aerosol optical thickness from 4-stream RT model at SZA = 25° and VZA = 0°. Different colors show SWARF as a function of surface albedo. The inset shows the relationship of SWARF and surface albedo.

tion of the positive and negative radiative effects making the SWDRE rather small.

[13] For the scattering mineral dust model, we calculate the SWDRE (the difference between TOA SWF in the absence and presence of aerosols) and analyze it as a function of surface albedo. Due to the close agreement between modeled and observed TOA SWF (Figure 2b), this analysis also holds for satellite observations. For each  $\alpha_s$  value, the clear sky value ( $F_{clr}$ ) is approximated as the SWF value where AOT = 0. Figure 3 shows the TOA SWDRE–AOT relation as a function of surface albedo (different colors). Using a linear regression on the modeled data we determine the slope of the SWDRE and AOT relation. This is defined as the dust radiative efficiency (DEFF). Negative slope indicates scattering (negative SWDRE) and positive slope indicates absorption (positive SWDRE) by aerosols. From Figure 3 we see that with the increase in surface albedo, the DEFF changes from negative to positive. The  $F_{clr}$ ,  $\alpha_s$ , SWDRE and DEFF values are tabulated in Table 1. From Table 1 we find that around the  $\alpha_c$  value (35%–40%), the positive and negative slope values are nearly equal and opposite and so are the SWDRE values, indicating that the dust SWDRE will be near zero over a region with a large range of albedo values. For example, for the selected mineral dust model in this study, the TOA SWDRE by dust aerosols over a region with albedo values ranging from 25–55% will be nearly zero (see the frequency distribution of surface albedo in Figure 1). This section describes a situation where only the selected scattering type mineral

dust is present over bright surface. In reality, there are more dust types present over deserts. Figures 2c and 2d, however, show that each of the 2 mineral dust types show similar effect on the SWF; the difference being in their  $\alpha_c$  values. These results show that the SWDRE of desert dust is rather small over bright land regions such as the Sahara desert where the broadband surface albedo ranges from 8–50% (Figure 1). Over bright land surfaces, the major contribution

**Table 1.** Top of Atmosphere Shortwave Direct Radiative Effect of Scattering Type Mineral Dust (Selected for This Study) From 4-Stream RT Model<sup>a</sup>

Albedo	F clr	F aero	SWDRE	DEFF	Y-Intercept
0.05	101.23	159.15	−65.04	−57.79	−2.43
0.10	141.49	192.84	−54.46	−49.43	−0.92
0.15	180.93	223.53	−45.11	−41.11	−0.57
0.20	220.72	254.64	−35.85	−32.87	−0.25
0.25	260.87	286.2	−26.69	−24.69	0.06
0.30	301.37	318.21	−17.63	−16.59	0.34
0.35	342.25	350.68	−8.69	−8.58	0.61
0.40	383.5	383.64	0.14	−0.66	0.86
0.45	425.13	417.11	8.83	7.15	1.08
0.50	467.16	451.09	17.38	14.86	1.29
0.55	509.6	485.61	25.79	22.45	1.47

<sup>a</sup>The first column shows the surface albedo values used in the RT model for top of the atmosphere (TOA) flux calculations.  $F_{clr}$  is the clear sky shortwave flux at TOA and DEFF is the dust radiative forcing efficiency which is the slope of the SWDRE–AOT linear regression line and Y-Intercept its intercept.

of these aerosols to DRE will be in the longwave [Zhang and Christopher, 2003].

#### 4. Summary and Conclusions

[14] The shortwave radiative effect of aerosols is best discernible for low reflectivity backgrounds and highly scattering aerosols. In this study, using satellite data and radiative transfer calculations, we have carefully quantified under what conditions we can see this change in shortwave flux due to changes in aerosol loading (as given by AOT) over the Sahara desert. This study offers observational evidences for the following statements:

[15] 1. The broadband SWDRE is not only dependent upon aerosol properties but is also very sensitive to the surface albedo. If the surface is very bright (35–40%), TOA shortwave fluxes do not respond substantially to an increase in aerosol loading and therefore the SWDRE is negligible.

[16] 2. There is a critical surface albedo below (above) which the scattering (absorption) effect of dust aerosol dominates. This critical surface albedo is a function of the aerosol properties and surface type. For a mixture of different dust types and for a range of surface albedo values, the negative and positive effects can compensate each other; resulting in small SWDRE values. Satellite observations used in this study can be used to estimate this critical albedo value.

[17] 3. While considering the dust radiative effects on climate, it is very crucial to have a proper knowledge of the underlying surface conditions, i.e., the surface albedo range. Over bright regions with scattering aerosols, aerosol concentration and properties show a second order effect.

[18] The major conclusion from this paper is that dust over high reflectance regions offers a scene with low contrast and hence does not enhance the TOA effective albedo substantially. Therefore, the TOA dust SWDRE over these regions will be small. Finally we note that in contrast to our previous studies over ocean where TOA dust SWDRE outweighs LWRE, over land the TOA SWDRE is negligible when compared to the LWRE. Dust also undergoes internal and external mixing with other aerosol species and therefore their radiative effects become important to both regional and global climate. If the sum of SWDRE and LWRE over oceans is negative, it remains to be seen if in a global sense the LWRE of dust over land will balance the SWDRE of dust over oceans.

[19] **Acknowledgments.** This research is supported by NASA's Radiation sciences, Interdisciplinary sciences, an EOS grant, and ACMAP programs. The data were obtained through the NASA Langley Distributed Active Archive Systems and other data sets.

#### References

Chen, Y., Q. Li, R. A. Kahn, J. T. Randerson, and D. J. Diner (2009), Quantifying aerosol direct radiative effect with Multiangle Imaging Spectroradiometer observations: Top-of-atmosphere albedo change by aerosols based on land surface types, *J. Geophys. Res.*, *114*, D02109, doi:10.1029/2008JD010754.

Christopher, S. A., P. Gupta, J. Haywood, and G. Greed (2008), Aerosol optical thicknesses over North Africa: 1. Development of a product for model validation using Ozone Monitoring Instrument, Multiangle Imaging Spectroradiometer, and Aerosol Robotic Network, *J. Geophys. Res.*, *113*, D00C04, doi:10.1029/2007JD009446.

Fu, Q., and K. N. Liou (1993), Parameterization of the radiative properties of cirrus clouds, *J. Atmos. Sci.*, *50*, 2008–2025, doi:10.1175/1520-0469(1993)050<2008:POTRPO>2.0.CO;2.

Greed, G., J. M. Haywood, S. Milton, A. Keil, S. Christopher, P. Gupta, and E. J. Highwood (2008), Aerosol optical depths over North Africa: 2. Modeling and model validation, *J. Geophys. Res.*, *113*, D00C05, doi:10.1029/2007JD009457.

Grini, A., and C. S. Zender (2004), Roles of saltation, sandblasting, and wind speed variability on mineral dust aerosol size distribution during the Puerto Rican Dust Experiment (PRIDE), *J. Geophys. Res.*, *109*, D07202, doi:10.1029/2003JD004233.

Haywood, J. M., et al. (2008), Overview of the Dust and Biomass-burning Experiment and African Monsoon Multidisciplinary Analysis Special Observing Period-0, *J. Geophys. Res.*, *113*, D00C17, doi:10.1029/2008JD010077.

Hess, M., P. Koepke, and I. Schult (1998), Optical Properties of Aerosols and Clouds: The software package OPAC, *Bull. Am. Meteorol. Soc.*, *79*, 831–844, doi:10.1175/1520-0477(1998)079<0831:OPOAAC>2.0.CO;2.

Hsu, N. C., S. C. Tsay, M. D. King, I. E. E. Senior Member, and J. R. Herman (2004), Aerosol properties over bright-reflecting source regions, *IEEE Trans. Geosci. Remote Sens.*, *42*(3), 557–569, doi:10.1109/TGRS.2004.824067.

Intergovernmental Panel on Climate Change (2007), *Climate Change 2007: The Physical Science Basis. Contribution of Working Group I to the Fourth Assessment Report of the Intergovernmental Panel on Climate Change*, edited by S. Solomon et al., Cambridge Univ. Press, Cambridge, U. K.

Johnson, B. T., S. R. Osborne, J. M. Haywood, and M. Harrison (2008), Aircraft measurements of biomass burning aerosol over West Africa during DABEX, *J. Geophys. Res.*, *113*, D00C06, doi:10.1029/2007JD009451.

Laurent, B., B. Marticorena, G. Bergametti, J. F. Léon, and N. M. Mahowald (2008), Modeling mineral dust emissions from the Sahara desert using new surface properties and soil database, *J. Geophys. Res.*, *113*, D14218, doi:10.1029/2007JD009484.

Liao, H., and J. H. Seinfeld (1998), Radiative forcing by mineral dust aerosols: Sensitivity to key variables, *J. Geophys. Res.*, *103*(31), 637–645.

McClatchey, R. A., R. W. Fenn, J. E. A. Selby, F. E. Volz, and J. S. Garing (1971), Optical properties of the atmosphere, *Environ. Res. Pap. 354*, Air Force Cambridge Res. Lab, Bedford, Mass.

Osborne, S. R., B. T. Johnson, J. M. Haywood, and C. L. McConnell (2008), Physical and optical properties of mineral dust aerosol during the Dust and Biomass-burning Experiment (DABEX), *J. Geophys. Res.*, *113*, D00C03, doi:10.1029/2007JD009551.

Patadia, F., P. Gupta, and S. A. Christopher (2008), First observational estimates of global clear sky shortwave aerosol direct radiative effect over land, *Geophys. Res. Lett.*, *35*, L04810, doi:10.1029/2007GL032314.

Prospero, J. M., P. Ginoux, O. Torres, S. Nicholson, and T. Gill (2002), Environmental characterization of global sources of atmospheric soil dust derived from the Nimbus 7 Total Ozone Mapping Spectrometer (TOMS) absorbing aerosol product, *Rev. Geophys.*, *40*(1), 1002, doi:10.1029/2000RG000095.

Schaaf, C. B., et al. (2002), First operational BRDF, albedo nadir reflectance products from MODIS, *Remote Sens. Environ.*, *83*, 135–148, doi:10.1016/S0034-4257(02)00091-3.

Yoshida, M., and H. Murakami (2008), Dust absorption averaged over the Sahara inferred from moderate resolution imaging spectroradiometer, *Appl. Opt.*, *47*, 1995–2003, doi:10.1364/AO.47.001995.

Zhang, J., and S. A. Christopher (2003), Longwave radiative forcing of dust aerosols over the Saharan Desert estimated from MODIS, MISR, and CERES observations from Terra, *Geophys. Res. Lett.*, *30*(23), 2188, doi:10.1029/2003GL018479.

S. A. Christopher, F. Patadia, and E.-S. Yang, Department of Atmospheric Sciences, University of Alabama in Huntsville, 320 Sparkman Drive, Huntsville, AL 35806-1912, USA. (falguni@nsstc.uah.edu)